JOURNAL OF CATALYSIS **161,** 377–386 (1996)
ARTICLE NO. 0195

Modeling of 2-Methylpentane Cracking: The Application of Adsorption Equilibrium Constants Estimated Using Proton Affinities

B. Sowerby,* S. J. Becker,† and L. J. Belcher‡

*School of Chemical Engineering, University of Bath, Claverton Down, Bath BA2 7AY, United Kingdom; †BP Chemicals Limited, Technology and Engineering Department, Middlesex TW16 7LL, United Kingdom; and ‡BP Oil International, Oil Technology Centre, Middlesex TW16 7LN, United Kingdom

Received February 15, 1995; revised February 16, 1996; accepted February 19, 1996

This article presents a practical approach for estimating adsorption equilibrium constants, K_p, for inclusion in Eley–Rideal type rate expressions, using van't Hoff's isochore equation, $RT\ln K_p = -\Delta H_{ad} + T\Delta S_{ad}$. The heats of adsorption, $-\Delta H_{ad}$, have been calculated using proton affinites and heats of condensation, and the entropy of adsorption, ΔS_{ad}, has been calculated using the Sackur–Tetrode equation. The equilibrium constants have been incorporated into a model for 2-methylpentane cracking that is based on a previously published reaction mechanism. The predicted behavior of the model compares well with published experimental data for a range of catalyst to oil ratios. This new model is also capable of predicting surface coverages of reaction intermediates; for an overall conversion of 10%, over 80% of the catalyst surface is covered with adsorbed C_6 olefin. In addition, the model predictions compare well with published experimental results for dilution of the feed stream with a nonpolar species such as nitrogen. © 1996 Academic Press, Inc.

INTRODUCTION

Fluid catalytic cracking (FCC) is a major unit operation when refining crude oil to produce high-quality gasoline. The need for accurate and fundamentally based process models is becoming more important in design and operability studies as profit margins are squeezed and as new environmental regulations must be met. One key decision when developing such process models is "What level of complexity should be implemented for the reaction mechanism and kinetic rate expressions?"

To date, because of the complexity of the problem, models that have been developed for FCC have been based on pseudo-components and simple power law rate expressions. These lumped parameter models have been used extensively and successfully for control and qualitative operability studies. Modern analytical techniques have made it possible to identify the individual species in FCC and recently a wealth of qualitative and semiempirical data has been published for a variety of model compounds on important features of FCC chemistry and operation such as deactivation by a progressive reduction in the number of acid sites (1), the poisoning effect of nitrogen compounds (2), and the inhibition effect of polar and nonpolar species (3).

To be able to quantitatively describe and predict the aforementioned phenomena and to be able to relate catalyst properties to unit operation performance, a more detailed description of the species involved as well as a better representation of the fundamental processes that are occurring between the bulk fluid and catalyst surface than that which is currently employed in pseudo-component, lumped parameter, power law models is required. This more fundamental approach to reaction modeling has been achieved in many systems where there are only a few components and reactions by using Langmuir–Hinshelwood- and/or Eley–Rideal-type rate expressions; such expressions are developed by considering the individual adsorption and reaction steps and are validated using a rigorously defined experimental programme (4). This approach is not particularly well suited to developing a more fundamentally based FCC model because of the large number of species, reactions, and thus adsorption and rate constants involved. To develop more fundamental FCC models on the basis of rate expressions that take into consideration the surface of the catalyst a more predictive approach for obtaining the adsorption and rate constants is required, but such an approach must be able to be validated using a limited but representative range of model compounds.

The work presented in this article has drawn on results and observations from a diverse source of published literature and in this article a practical approach for estimating adsorption equilibrium constants, K_p, for inclusion in Langmuir–Hinshelwood- and/or Eley–Rideal-type rate expressions is presented. To test the proposed approach, the estimated equilibrium constants have been incorporated into a model for 2-methylpentane cracking that is based on a previously published reaction mechanism. The predicted behavior of the model is compared quantitatively with published experimental data for 2-methylpentane cracking and qualitatively with published experimental and modeling

0021-9517/96 $18.00

data for isobutane cracking. Predicted concentrations of components on the catalyst surface and the consequence of diluting the 2-methylpentane feed with nitrogen, carbon monoxide, and carbon dioxide are also presented.

METHOD

Reaction Mechanism and Kinetics

In the model presented here, the reaction mechanism for 2-methylpentane cracking proposed by Zhao *et al.* (5) has been used. The mechanism proposed consists of the sequential steps described below.

1. Monomolecular reactions. Reactions are initiated by adsorption of 2-methylpentane feed onto Brønsted acid sites; thus the paraffin undergoes protonation and a carbonium ion is formed

$$C_6H_{14} + H^+ \rightarrow C_6H_{15}^+,$$

where H^+ is a Brønsted acid site. Subsequent protolysis produces a carbenium ion on the surface of the catalyst and a smaller gas-phase paraffin molecule

$$C_6H_{15}^+ \rightarrow C_nH_{2n+1}^+ + C_{6-n}H_{14-2n} \quad \text{with } n = 0, 1, 2, 3, 4, 5, 6,$$

where $C_nH_{2n+1}^+$ is the carbenium ion on the surface of the catalyst (an adsorbed protonated olefin) and $C_{6-n}H_{14-2n}$ is the paraffin or hydrogen molecule ($n = 0$) released into the gas phase.

2. Bimolecular reactions. Propagation reactions occur by hydride transfer between carbenium ions on the surface of the catalyst and gas-phase feed molecules. These reactions can be decomposed into the following two steps:

(i) hydride transfer using the carbenium ion

$$C_6H_{14} + C_nH_{2n+1}^+ \rightarrow C_6H_{13}^+ + C_nH_{2n+2}$$

(ii) β-scission of the carbenium ion

$$C_6H_{13}^+ \rightarrow C_nH_{2n+1}^+ + C_{6-n}H_{12-2n}.$$

Zhao *et al.* (5) experimentally determined certain bimolecular reactions to be more significant than others, and the most significant ones have been implemented in this model.

3. Desorption. Reactions are terminated by the decomposition of carbenium ions to yield a gas-phase olefin molecule by desorption and to leave a free Brønsted acid site on the catalyst

$$C_nH_{2n+1}^+ \rightleftarrows C_nH_{2n} + H^+ \quad \text{with } n = 2, 3, 4, 5, 6.$$

4. Isomerization. Carbenium ions adsorbed on the surface can rearrange to form skeletal isomers

$$C_6H_{13}^+ \rightarrow \text{i-}C_6H_{13}^+$$

and this is then followed by a rate controling bimolecular hydride transfer step

$$C_6H_{14} + \text{i-}C_6H_{13}^+ \rightarrow \text{i-}C_6H_{14} + C_6H_{13}^+.$$

The β-scission of isomerized products has not been taken into account here.

The complete reaction mechanism implemented is given in Table 1. Catalyst deactivation by coke laydown has

TABLE 1

Reactions and Rate Expressions for 2-Methylpentane Cracking

Reaction	Rate expression
Protonation and protolysis	
1. $C_6H_{14} + H^+ \rightarrow H_2 + C_6H_{13}^+$,	$r_1 = k_1 K_{p_{C_6H_{14}}} p_{C_6H_{14}}/(1 + \Sigma K_{p_i} p_i)$
2. $C_6H_{14} + H^+ \rightarrow CH_4 + C_5H_{11}^+$,	$r_2 = k_2 K_{p_{C_6H_{14}}} p_{C_6H_{14}}/(1 + \Sigma K_{p_i} p_i)$
3. $C_6H_{14} + H^+ \rightarrow C_2H_6 + C_4H_9^+$,	$r_3 = k_3 K_{p_{C_6H_{14}}} p_{C_6H_{14}}/(1 + \Sigma K_{p_i} p_i)$
4. $C_6H_{14} + H^+ \rightarrow C_3H_8 + C_3H_7^+$,	$r_4 = k_4 K_{p_{C_6H_{14}}} p_{C_6H_{14}}/(1 + \Sigma K_{p_i} p_i)$
5. $C_6H_{14} + H^+ \rightarrow C_4H_{10} + C_2H_5^+$,	$r_5 = k_5 K_{p_{C_6H_{14}}} p_{C_6H_{14}}/(1 + \Sigma K_{p_i} p_i)$
Hydride transfer and β-scission	
6. $C_6H_{14} + C_2H_5^+ \rightarrow C_5H_{12} + C_3H_7^+$,	$r_6 = k_6 K_{p_{C_2H_4}} p_{C_6H_{14}} p_{C_2H_4}/(1 + \Sigma K_{p_i} p_i)$
7. $C_6H_{14} + C_3H_7^+ \rightarrow C_3H_8 + C_6H_{13}^+$,	$r_7 = k_7 K_{p_{C_3H_6}} p_{C_6H_{14}} p_{C_3H_6}/(1 + \Sigma K_{p_i} p_i)$
8. $C_6H_{14} + C_2H_5^+ \rightarrow C_4H_{10} + C_4H_9^+$,	$r_8 = k_8 K_{p_{C_2H_4}} p_{C_6H_{14}} p_{C_2H_4}/(1 + \Sigma K_{p_i} p_i)$
9. $C_6H_{14} + C_3H_7^+ \rightarrow C_5H_{12} + C_4H_9^+$,	$r_9 = k_9 K_{p_{C_3H_6}} p_{C_6H_{14}} p_{C_3H_6}/(1 + \Sigma K_{p_i} p_i)$
10. $C_6H_{14} + C_5H_{11}^+ \rightarrow C_5H_{12} + C_6H_{13}^+$,	$r_{10} = k_{10} K_{p_{C_5H_{10}}} p_{C_6H_{14}} p_{C_5H_{10}}/(1 + \Sigma K_{p_i} p_i)$
Isomerization (carbenium ion rearrangement plus β scission)	
11. $C_6H_{14} + C_6H_{13}^+ \rightarrow \text{i-}C_6H_{14} + C_6H_{13}^+$,	$r_{11} = k_{11} K_{p_{C_6H_{12}}} p_{C_6H_{14}} p_{C_6H_{12}}/(1 + \Sigma K_{p_i} p_i)$,
where $(1 + \Sigma K_{p_i} p_i) = 1 + K_{p_{C_6H_{14}}} p_{C_6H_{14}} + K_{p_{C_2H_4}} p_{C_2H_4} + K_{p_{C_3H_6}} p_{C_3H_6} + K_{p_{C_4H_8}} p_{C_4H_8} + K_{p_{C_5H_{10}}} p_{C_5H_{10}} + K_{p_{C_6H_{12}}} p_{C_6H_{12}}$	

been accounted for by implementing the following time on stream-dependent deactivating function used by Zhao *et al.* (5)

$$Q_{\text{acid}}|_t = Q_{\text{acid}}|_{t=0}/(1 + 0.262t), \quad [1]$$

where $Q_{\text{acid}}|_t$ is the total number of acid sites available at time t, $Q_{\text{acid}}|_{t=0}$ is the total number of acid sites initially available, and t is the time on stream in minutes. Coke formation by carbenium ion polymerization has not been included at this stage.

In the hydride transfer steps of the bimolecular and isomerization reactions described above, it has been assumed that reaction occurs between an adsorbed molecule and a gas-phase molecule; thus Eley–Rideal kinetic rate expressions are the most appropriate for describing these reaction rates. The rate expressions used in this work are given in Table 1 and their full derivation is given in the Appendix.

Equilibrium Constants

A key parameter in the rate expressions developed is the adsorption equilibrium constant K_p. In the model presented here, this constant will dictate the relative amount of each species on the surface of the catalyst.

The adsorption of paraffins in medium pore zeolites is described well by Langmuir isotherms. Completely reversible equilibrium is exhibited and coverages are independent of the heat of adsorption. The adsorption equilibrium constant can therefore be estimated using van't Hoff's equation

$$\frac{d(\ln K_p)}{dT} = \frac{\Delta H_{\text{ad}}}{RT^2}. \quad [2]$$

where ΔH_{ad} is the enthalpy of adsorption, T is temperature, and R is the universal gas constant.

The overall energy associated with adsorption of paraffins onto zeolite surfaces has traditionally been thought to be composed of two factors; the first is that associated with the inherent proton donating ability of the acid site to the paraffin and the second the stabilization energy of the molecule inside the zeolite lattice. To enable the heat of adsorption to be calculated, ultimately for a wide range of FCC components, a method of estimating of these two factors using published physical and chemical property data is required. Here, they have been estimated using the energies associated with proton transfer and condensation, respectively. Thus, the overall energy associated with the adsorption of paraffins onto a zeolite surface has been estimated by combining the energies associated with proton transfer and condensation. These two energies have been combined together using an analogous approach to that used for combining activation energies of sequential diffusion and rate processes (7); that is, the overall energy is equal to half the sum of the constituent energies,

$$\Delta H_{\text{ad}} = \frac{(\text{PA} - \text{PA}_{\text{min}}) + \Delta H_{\text{c}}}{2} \quad [3]$$

TABLE 2

Proton Affinities, Heats of Condensation, and Equilibrium Constants

Component	Proton affinity, PA (kJ/mol)	Heat of cond. $-\Delta H_{\text{c}}$, (kJ/mol)	Equilibrium constant, K_p
Hydrogen	628	0.91	0.191×10^{-32}
Methane	628	8.19	0.366×10^{-9}
Ethane	628	14.72	0.175×10^{-8}
Propane	683	14.84	0.515×10^{-8}
Butane	683	20.62	0.123×10^{-7}
Pentane	683	26.29	0.258×10^{-7}
2-Me-pentane	683	31.56	0.506×10^{-7}
C_6 Isomers	683	29.12	0.325×10^{-9}
Ethylene	720	13.55	0.151×10^{-4}
Propene	720	14.12	0.463×10^{-4}
Butene	835	19.60	0.302×10^{-3}
Pentene	848	25.07	0.109×10^{-2}
Hexene	855	30.35	0.317×10^{-2}
N_2	0	0.55	≈ 0
CO_2	595	17.17	1.400×10^{-11}
CO	547	1.40	4.700×10^{-14}

where PA is the proton affinity for the adsorbate, PA_{min} is the proton affinity for the catalyst, and ΔH_{c} is the enthalpy of condensation. In Eq. [3], it has been assumed that all of the proton charge is donated to the carbonium ion; this may not in fact be the case but is deemed a valid initial assumption. This simplified approach enables the heat of adsorption to be calculated for all component molecules using published properties.

Values for PA for the various components in the model have been obtained from standard heat of ionization tables (8). The values used here are given in Table 2. The standard heat of condensation at 25°C used for each component is also given in Table 2.

The proton affinity for the catalyst, that is, the acid site strength, is dependent on the catalyst used. For a particular catalyst all sites may have the same acid strength; that is, one value for PA_{min} or a range of acid site strengths may exist. Recently, when Parillo *et al.* (9) related the heat of adsorption to the proton affinity for the adsorption of a series of simple amines on ZSM-5, they found that a single acid site strength of 712 kJ/mol adequately described their experimental data. In addition, when Chen *et al.* (6) studied the acidity characteristics of ZSM-5, H mordenite, and HY zeolites by microcalorimetric and gravimetric measurements of pyridine adsorption, they confirmed that ZSM-5 (and in fact H mordenite as well) has Brønsted acid sites of a primarily homogeneous strength of 764 kJ/mol, whereas HY zeolite has Brønsted sites of varying strengths 744–794 kJ/mol. These acid site strengths have been determined using the heats of adsorption given by Chen *et al.* and a proton affinity of 924 kJ/mol for pyridine.

Thus, making use of Eq. [3], the adsorption constant, K_p, for any component of known molecular weight, proton

affinity, and heat of condensation can be estimated using the following integrated form of Eq. [2]

$$K_p = \exp\left\{ \frac{(\mathrm{PA} - \mathrm{PA}_{\min}) + \Delta H_c}{2RT} + \frac{\Delta S_{ad}}{R} + C_1 \right\}, \quad [4]$$

where ΔS_{ad} is the entropy of adsorption and C_1 is an additional constant of integration.

The entropy of adsorption of molecules on an acid catalyst is, like the enthalpy of adsorption, a combination of two factors. As a molecule adsorbs from the gas phase onto an acid site there is a partial loss in translational and perhaps also rotational degrees of freedom. The entropy of an adsorbed molecule is also a function of the resultant mobility of the molecule. Here the entropy of adsorption has been assumed to be equal to the loss of all the translational degrees of freedom of the vapor molecule. The Sackur and Tetrode equation (10) has been used to estimate the loss in translational freedom

$$\Delta S_{ad} = R \ln\left\{ \frac{e^{5/2} V}{L h^3} (2\pi m k T)^{3/2} \right\}, \quad [5]$$

where R is the universal gas constant, V is the gas molar volume, L is Avogadro's constant, h is Planck's constant, m is the mass of one particle, k is Boltzmann's constant, and T is temperature.

The constant of integration, C_1, has been estimated as 29.1 using the data of Maatman *et al.* (11), who measured equilibrium constants for the adsorption of hydrocarbons on silica-alumina over a range of temperatures. They also calculated enthalpies and entropies of adsorption on cracking sites.

For a catalyst with a homogeneous acid site strength of 712 kJ/mol, the equilibrium constants at 400°C calculated using Eq. [4] are given in Table 2.

Reactor Model

The reaction mechanism and rate expressions have been incorporated into an isothermal fixed bed reactor model. In such a model the rate of change of each component along the length of the reactor is given by

$$\frac{dF_i}{dz} = \Sigma_j a_{ij} r_j, \quad [6]$$

where F_i is the flow rate of component i, z is the axial length, a_{ij} is the stoichiometric coefficient for component i in reaction j, and r_j is the rate of reaction j.

The component flow rates along the length of the reactor have been calculated by integrating Eq. [6]. The fraction of the acid sites or catalyst surface occupied by each component at each axial increment was calculated using

$$Q_i|_z = K_{p_i} p_i|_z / \Sigma_i K_{p_i} p_i|_z, \quad [7]$$

where $Q_i|_z$ is the catalyst loading for component i at position z along the reactor and $p_i|_z$ is the gas-phase partial pressure for component i at position z along the reactor.

Experimental Data

The reaction rate constants for 2-methylpentane cracking have been established by matching predicted reactor performance to the experimental data published by Zhao *et al.* (5, 12). A brief overview of the experimental procedure and analysis of results is given in this section, but full details are given in Ref. (13).

The cracking of 2-methylpentane was studied experimentally using a fixed bed gas-phase plug flow reactor (0.02 m i.d. and 0.15 m long) packed with HY zeolite catalyst, mesh size 50/70. The HY zeolite catalyst (97.3% exchanged) had been prepared from NaY by repeated exchange with 0.5 *M* ammonium nitrate solution. The catalyst was diluted in the bed in order to maintain isothermal operation. Before a reaction run the bed was purged with nitrogen gas. Immediately after the purge period a measured amount of pure reactant was pumped through the reactor. The reactant was vaporized and heated up to the reactor temperature in a preheating section and then converted in the catalyst bed. All experiments were carried out at 400°C and at 1 atm pressure. The reaction products were analyzed by gas chromatography. Experiments were performed at various catalyst to oil ratios. The raw experimental data were manipulated to remove the contribution of thermally cracked products. Thus, product distributions for pure catalytic cracking of 2-methylpentane were presented as a plot of conversion versus time on stream for various catalyst to oil ratios, and plots of weight percent of each major component in the product versus weight percent conversion of the feed. Some of these results are given in Figs. 1 and 2.

RESULTS AND DISCUSSION

Predicted Data

The reaction rate constants $k_1, k_2, \ldots, k_{11}$ defined by the rate expressions given in Table 1 have been established by matching model predictions to experimental data. The total number of acid sites initially available was assumed to be 5×10^{19} sites/g as established by Cardona-Martinez and Dumesic (15). The absolute value of the number of sites is not significant in this particular model as it is present in all rate expressions. It has been included here for completeness and for future studies where the number of acid sites may vary as discussed later in this article.

The behavior predicted by the model is compared with the experimental data in Figs. 1 and 2. The figures show that the model predicts the correct variation in overall conversion of 2-methylpentane with time on stream for various catalyst to oil ratios. This is as expected, since in this

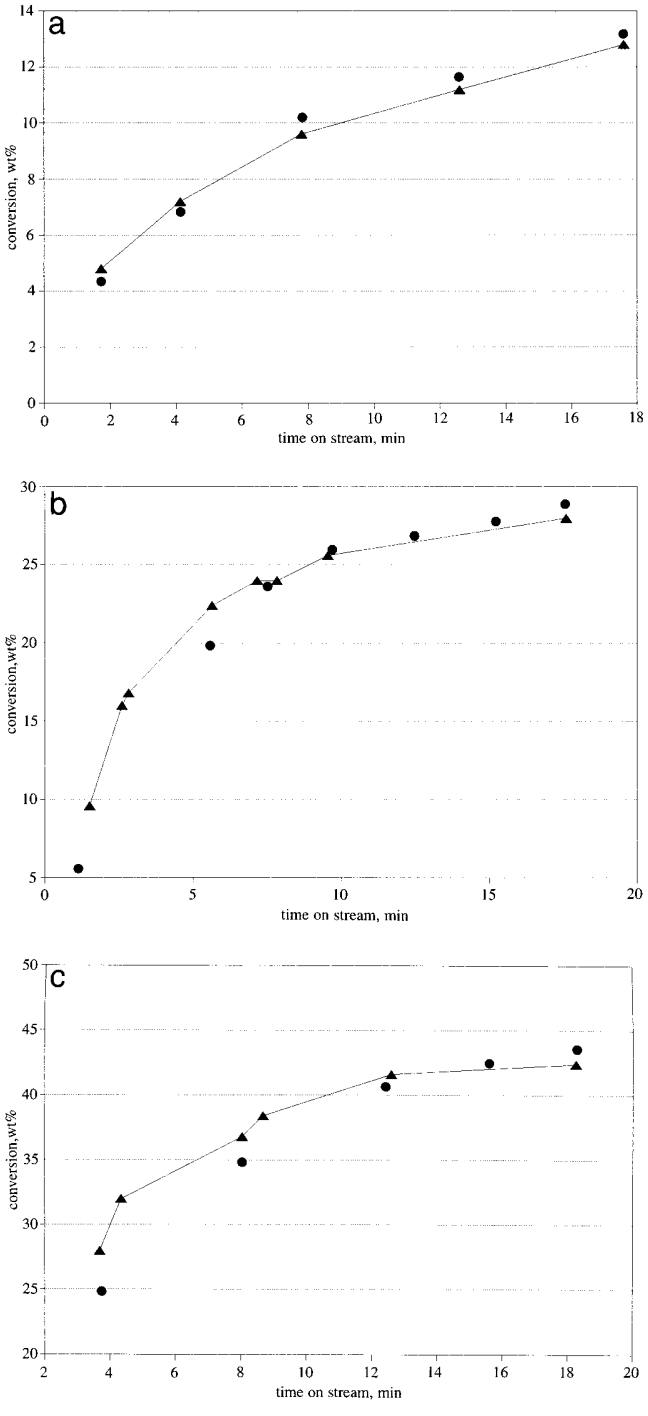

FIG. 1. Variation in overall conversion of 2-methyl-pentane with time on stream for various catalyst to oil ratios. (a) Cat : oil = 0.0077; (b) cat : oil = 0.043; (c) cat : oil = 0.104. (-▲-) experimental; (●) predicted.

model, catalyst deactivation by coke formation is accounted for by Eq. [1] and this equation was determined by Zhao *et al.* (5) by fitting to experimental data. However, the model presented here with no further adjustment of reaction parameters is capable of predicting the correct trend in product distribution with conversion, although in a few cases the absolute magnitude in variation is not always precisely correct. If either the reaction mechanism or the relative magnitude of the adsorption equilibrium constants was not representative then this would not have been the case. Previously when modeling these data, Zhao *et al.* (3, 5, 12) lumped together the adsorption equilibrium constant and reaction rate constant for each reaction. The present new procedure for estimating adsorption equilibrium constants enables these two model parameters to be separated but perhaps more importantly enables surface coverages to be predicted and thus compared with earlier speculated findings.

Surface Coverages

The variation in surface coverage of carbonium ion and carbenium ion intermediates along the length of the reactor with conversion has been calculated using Eq. [7]. For conversions of 10 and 40% the resultant surface coverages are shown in Figs. 3 and 4, respectively.

In Fig. 3, it is shown that once the profiles are established, then, for an overall conversion of 10%, approximately 80% of the surface is covered with adsorbed protonated C_6 olefin, that is, the carbenium ion $C_6H_{13}^+$. This is in agreement with Zhao *et al.*'s (5) statement that the products of 2-methylpentane cracking are more strongly adsorbed on the active sites relative to the feed molecules. In Fig. 3, it is also shown, as expected, that at the front of the reactor the surface concentration of the feed is initially high and then rapidly decreases in an exponential fashion. This exponential decline in the surface concentration of the feed is accompanied first by an increase in the coverage of initiation reaction products, that is, C_2, C_3, C_4, and C_5 olefins, and then by an increase in the coverage of propagation reaction products. The surface coverage profiles of the primary products that are then consumed by propagation reactions all exhibit a maximum value as the initial increasing trend in surface concentration due to an initiation reaction is reversed when the concentrations are such that propagation reactions begin to dominate. It should be pointed out that, in the model presented here, catalyst deactivation due to coke laydown has been described using Eq. [1], which gives a uniform decay along the length of the reactor. Catalyst deactivation due to the adsorption of product olefins in the form of carbenium ions progressively increases along the length of the reactor. Had coke formation by olefin polymerization been included in the model, then deactivation by coke laydown would also have increased with axial distance.

The surface coverages for the higher-conversion case shown in Fig. 4 exhibit trends similar to those of the low conversion case shown in Fig. 3. However, in the high-conversion case a less clearly defined maximum in the olefin products is observed. This is because the effects of the now much faster propagation reactions dominate the form of the resultant profiles.

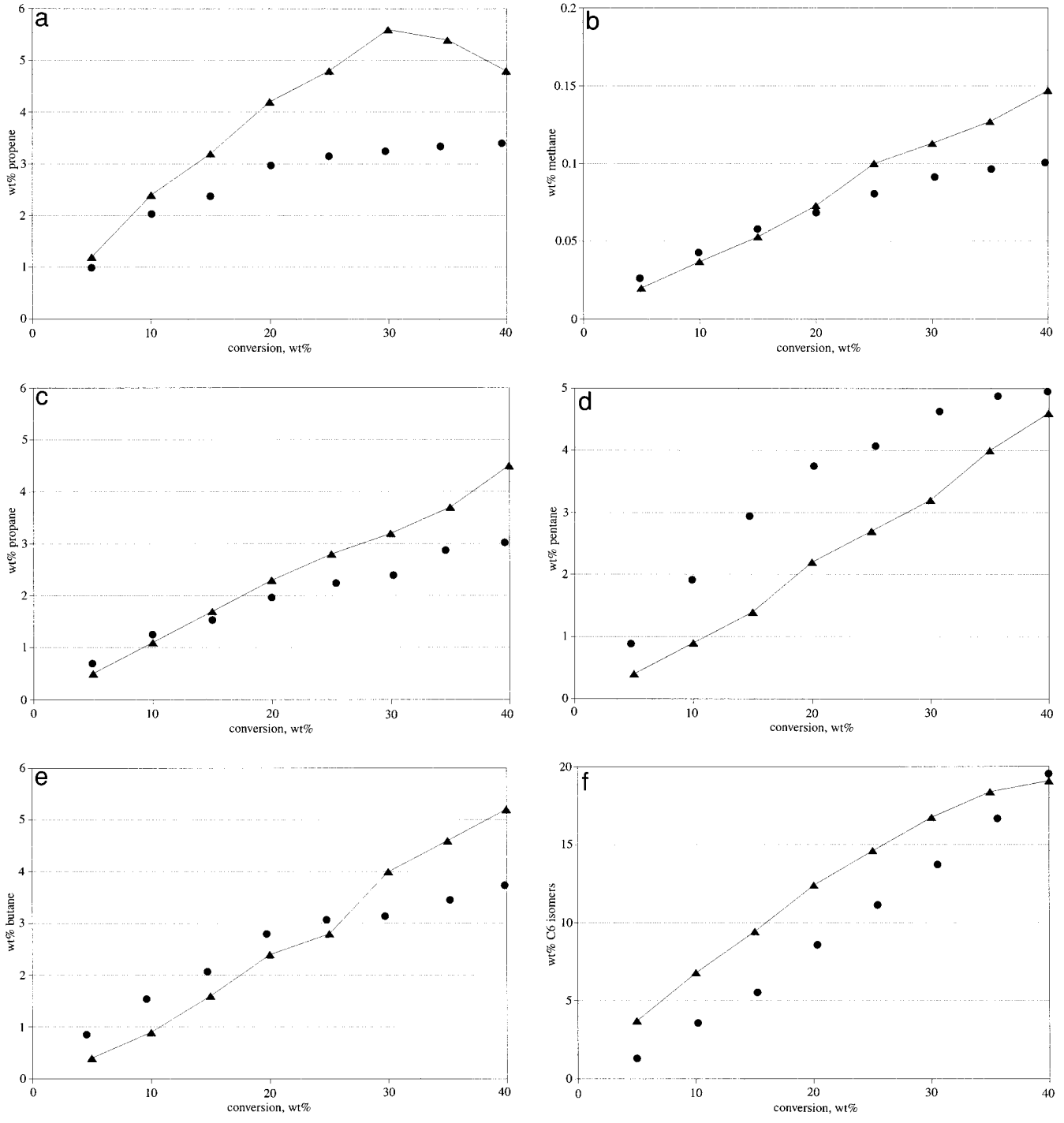

FIG. 2. Variation in weight percentage of various products vs overall conversion. (a) Propene; (b) methane; (c) propane; (d) pentane; (e) butane; (f) C_6 isomers. (-▲-) experimental; (●) predicted.

The relative rates of reaction for the 40% conversion case are plotted in Fig. 5. Figure 5 shows that the initiation reactions 4 and 5 are the dominant ones in that class. Their rates steadily decline along the length of the reactor as the gas-phase concentration of the 2-methylpentane feed decreases. Within the propagation class of reactions, reaction 6 dominates because of its high reactant concentration, viz. adsorbed protonated C_2 olefin. The then steady decline in this reaction rate can also be attributed to decline in the gas-phase concentration of the feed.

These predicted reaction rates are in general agreement with those reported in a modeling study of isobutane

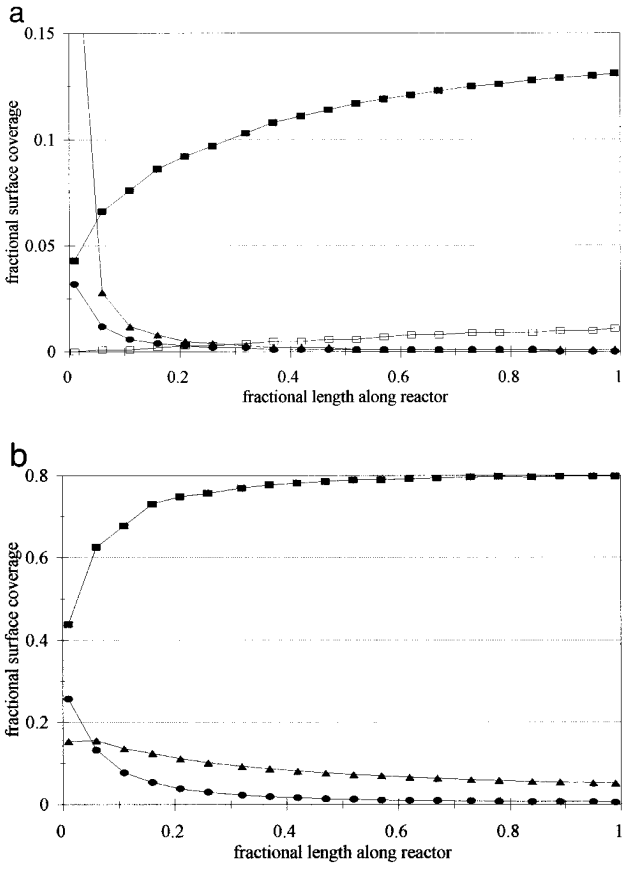

FIG. 3. Variation in fractional surface coverages of adsorbed protonated olefins with fractional length along reactor for an overall 2-methylpentane conversion of 10%. (a) -▲-, $C_6H_{13}^+$; -●-, $C_2H_5^+$; -■-, $C_4H_9^+$; -□-, $C_6H_{13}^+$; isomers. (b) -▲-, $C_3H_7^+$; -●-, $C_5H_{11}^+$; -■-, $C_6H_{13}^+$.

cracking (14). A microkinetic model of isobutane cracking with a similarly structured reaction mechanism to the one implemented in the model here predicted that the net rate of initiation reactions is essentially constant along the length of the reactor whereas hydride transfer and the oligomerization rearrangement reactions are all negligible at the beginning of the reactor but become more dominant along the reactor. In the published work on isobutane cracking it was speculated that over a steamed Y-zeolite catalyst hydride transfer and oligomerization reactions are not as important because a steamed catalyst has weaker acid sites. However, steaming a catalyst may reduce the number of acid sites and thus reduce the contribution of bimolecular reactions. These different ideas could be readily investigated using the model presented here as acid site strength is represented in the model by the parameter PA_{min}, the number of acid sites is expressed explicitly, and a distribution of acid site strength can be represented by a range of PA_{min}'s.

Dilution of Feed

The introduction of a diluent gas into the 2-methylpentane feed can affect the rates of the reactions in a variety of ways. In the proposed reaction mechanism and rate expressions the reaction rates are dependent on the strength, distribution, activity, and concentration of active sites as well as on the partial pressure of the reactant in the gas phase. Thus, when a diluent is added to the feed it will most definitely decrease the partial pressure of the reactant but a diluent added to the feed may or may not also change the concentration of the active sites by preferentially adsorbing onto sites and/or change the apparent acid site strength by interacting with the adsorbing species.

Zhao and Wojciechowski (3) experimentally investigated the effect of diluents on 2-methylpentane cracking. A selection of their results for nitrogen, carbon dioxide, and carbon monoxide diluents is given in Fig. 6. It can be seen from these data, and indeed the authors themselves concluded, that for the same dilution ratio the different diluents reduce the overall conversion of feed by different extents. The order of the effect was seen to be

$$CO > CO_2 > N_2.$$

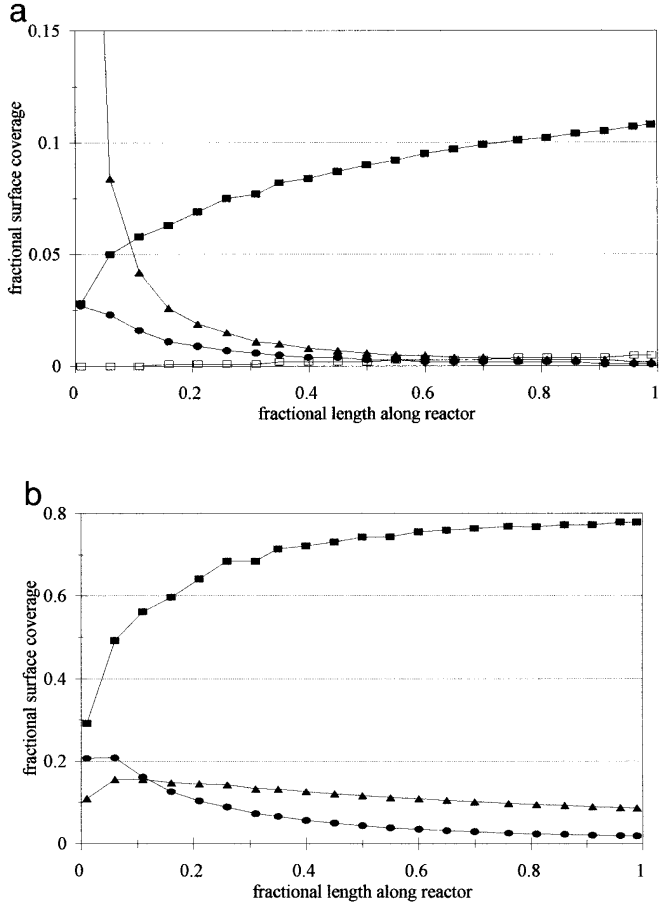

FIG. 4. Variation in fractional surface coverages of adsorbed protonated olefins with fractional length along reactor for an overall 2-methylpentane conversion of 40%. (a) -▲-, $C_6H_{13}^+$; -●-, $C_2H_5^+$; -■-, $C_4H_9^+$; -□-, $C_6H_{13}^+$ isomers. (b) -▲-, $C_3H_7^+$; -●-, $C_5H_{11}^+$; -■-, $C_6H_{13}^+$.

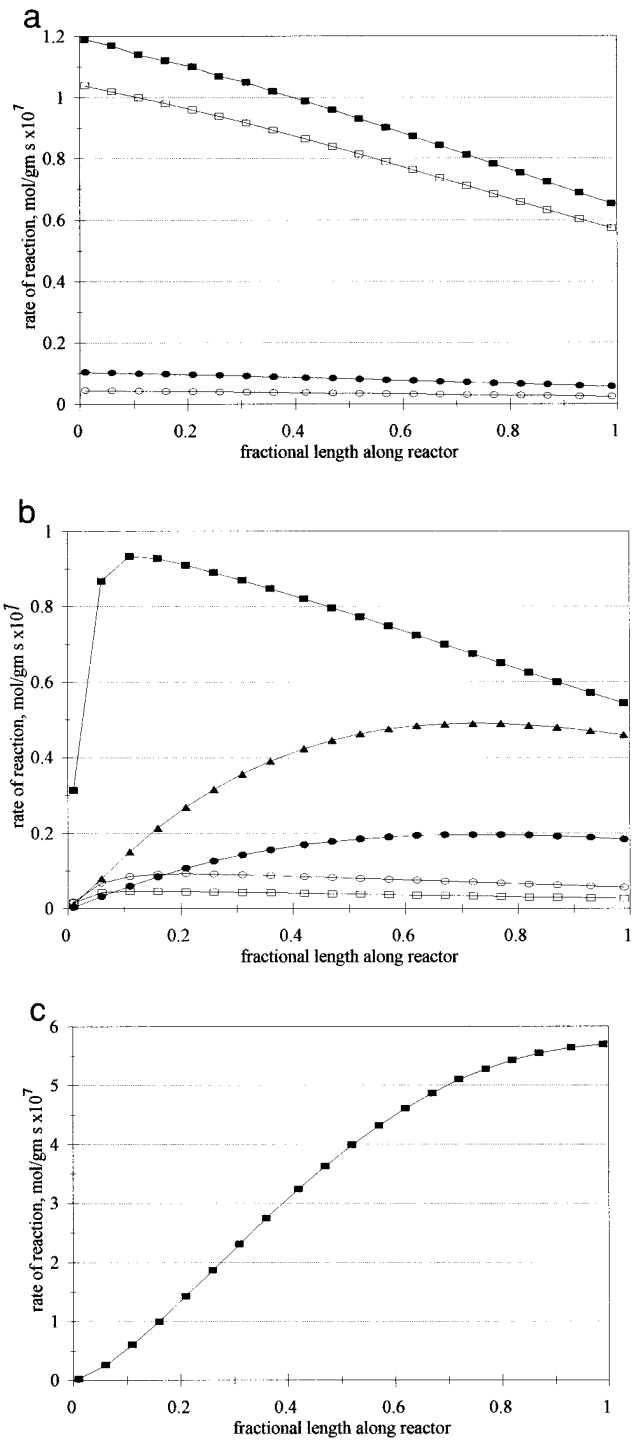

FIG. 5. Variation in individual reaction rates with axial distance for 40% conversion. (a) Initiation reactions: -●-, reaction 2; -○-, reaction 3; -■-, reaction 4; -□-, reaction 5. (b) Propagation reactions: -■-, reaction 6; -●-, reaction 7; -□-, reaction 8; -▲-, reaction 9; -○-, reaction 10. (c) Isomerization reaction: -■-, reaction 11.

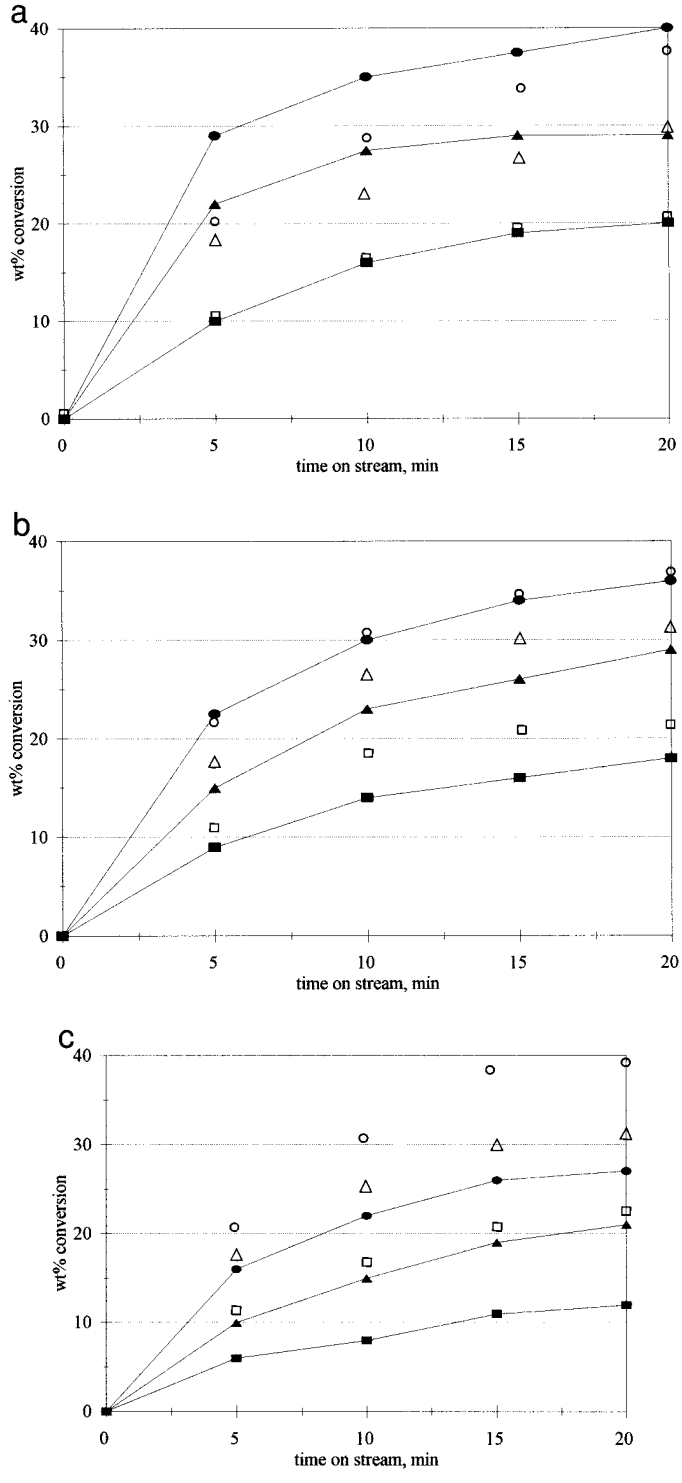

FIG. 6. Variation in weight percentage conversion of 2-methylpentane with time on stream for N_2, CO and CO_2 diluents and for various catalyst to oil ratios. (a) N_2; (b) CO; (c) CO_2. Cat : oil = 0.11: -●-, experimental; -○-, predicted. Cat : oil = 0.068: -▲-, experimental; -△-, predicted. Cat : oil = 0.035: -■-, experimental; -□-, predicted.

Zhao and Wojciechowski substantiated their experimental findings by fitting their lumped parameter model (3) to the experimental data. They found that in order to fit the experimental data adequately it was necessary to very all four of the model's lumped parameters, A_1, A_2, B, and G. In their model, A_1 relates the sum of the extent of monomolecular and bimolecular reactions, A_2 is representative of the rate of only bimolecular reactions, B quantifies the competition for adsorption sites between product olefin and feed species, and G is the catalyst deactivation constant. They concluded that

- the more polar the diluent then the more pronounced its passivation effect on the catalyst active sites
- diluents promote the decomposition of carbenium ions
- diluents decrease the reactivity of the carbenium ions.

In the model of 2-methylpentane cracking presented in this article, the behavior of nitrogen, carbon monoxide, and carbon dioxide has been described in the same manner as for all the hydrocarbons in the system, that is, using the molecular proton affinity and then calculating the equilibrium constant K_p using Eq. [4]. The proton affinities for N_2, CO, and CO_2 and the calculated K_p's are given in Table 2. The predicted effect of adding these diluents to the feed using the model presented here is shown in Fig. 6.

Figure 6 shows that the predicted effect when nitrogen is used as a diluent in the feed agrees well with that observed experimentally. However, Fig. 6 also shows that the predicted behavior of CO and CO_2 diluents in the feed is not in as good agreement as that seen for N_2. This is because in the model presented here CO and CO_2 are not capable of adsorbing on the active sites of the catalyst; their PA's are less than the PA_{min} for the catalyst, but the experimental results presented by Zhao and Wojciechowski (3) show that CO and CO_2 have a greater effect on the overall rate of 2-methylpentane cracking than N_2. If the reaction mechanism, rate expressions, and adsorption constant calculations are all correct, then as speculated by Zhao and Wojciechowski (3), CO and CO_2 must deactivate the catalyst in some way other than by adsorption onto free active catalyst sites. Zhao and Wojciechowski suggested that CO and CO_2 somehow decrease the reactivity of the carbenium ions and/or promote the desorption of carbenium ions. In fact, it has been shown by Koch and Haaf (16) that olefins can react with CO in the presence of an acid catalyst to form carboxylic acids. The first stage of this reaction pathway could be occurring here; the acid catalyst donates a proton to the olefin to which CO is then added forming an acyl ion:

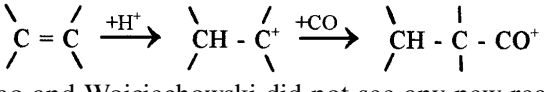

Zhao and Wojciechowski did not see any new reaction products when diluents were added to the feed. Thus, this bonding between an adsorbed olefin on an acid site and carbon monoxide could be the cause of the deactivation that they observed.

CONCLUSIONS

Adsorption equilibrium constants have been estimated using van't Hoff's equation. The heats of adsorption have been calculated using proton affinities and heats of condensation. The entropy of adsorption has been calculated using the Sackur–Tetrode expression.

The adsorption equilibrium constants have been implemented in a model for 2-methylpentane cracking. The reaction mechanism adopted in the model has been based on one proposed in the literature. Here, the adsorption and reaction processes have been kept distinct and not lumped as has been the practice by other workers.

The reaction model presented is capable of describing 2-methylpentane cracking over a range of catalyst to oil ratios. It was predicted that for an overall conversion of 10% then over 80% of the surface of the catalyst would be covered with adsorbed C_6 olefin ($C_6H_{13}^+$ carbenium ion). Because of the relatively high adsorption equilibrium constants of the product olefins with respect to the feed paraffin, the surface of the catalyst is in fact dominated by product olefins once they are present in sufficient concentration in the gas phase.

The model presented is also capable of quantifying the effect of diluting the feed stream with a nonpolar, nonreactive species such as nitrogen. However, in the case of dilution with a polar species, it is speculated that some polar species are able to react with the adsorbed protonated olefins. Currently this behavior is not included in the reaction mechanism and hence the model cannot accurately predict the effects of polar species such as CO and CO_2.

APPENDIX: DERIVATION OF RATE EXPRESSIONS

If it is assumed that equilibrium exists between all gas-phase and adsorbed-phase species then for the 2-methylpentane feed

$$C_6H_{14} + H^+ \rightleftarrows C_6H_{15}^+ \qquad [A.1]$$

and for the olefin products

$$C_6H_{13}^+ \rightleftarrows C_6H_{12} + H^+ \qquad [A.2]$$

$$C_6H_{11}^+ \rightleftarrows C_5H_{10} + H^+ \qquad [A.3]$$

$$C_6H_9^+ \rightleftarrows C_4H_8 + H^+ \qquad [A.4]$$

$$C_6H_7^+ \rightleftarrows C_3H_6 + H^+ \qquad [A.5]$$

$$C_6H_5^+ \rightleftarrows C_2H_4 + H^+. \qquad [A.6]$$

Applying the Langmuir adsorption model to the adsorption/desorption processes given above, the rate of adsorption $= k_a p_i Q_s$ and the rate of desorption $= k_d Q_i$, where k_a is the adsorption rate constant, k_d is the desorption rate constant, p_i is the gas-phase partial pressure of

component i, Q_s is the amount of free surface, and Q_i is the surface coverage of component i. At equilibrium, the rate of adsorption is equal to the rate of desorption, so the equilibrium constant, K_{p_i}, is given by,

$$K_{p_i} = k_a/k_d = Q_i/p_i Q_s, \quad [A.7]$$

where $i = C_6H_{14}$, C_6H_{12},C_5H_{10}, C_4H_8, C_3H_6, C_2H_4.

Monomolecular initiation reactions comprise adsorption of 2-methylpentane feed onto free acid sites; the paraffin undergoes protonation and a carbonium ion is formed then subsequent protolysis produces a carbenium ion on the surface of the catalyst. The overall monomolecular reactions and their rates are given by

$$C_6H_{15}^+ \rightarrow H_2 + C_6H_{13}^+,$$
$$r_1 = k_1 Q_{C_6H_{14}} = k_1 K_{p_{C_6H_{14}}} p_{C_6H_{14}} Q_s \quad [A.8]$$
$$C_6H_{15}^+ \rightarrow CH_4 + C_6H_{11}^+,$$
$$r_2 = k_2 Q_{C_6H_{14}} = k_2 K_{p_{C_6H_{14}}} p_{C_6H_{14}} Q_s \quad [A.9]$$
$$C_6H_{15}^+ \rightarrow C_2H_6 + C_6H_9^+,$$
$$r_3 = k_3 Q_{C_6H_{14}} = k_3 K_{p_{C_6H_{14}}} p_{C_6H_{14}} Q_s \quad [A.10]$$
$$C_6H_{15}^+ \rightarrow C_3H_8 + C_6H_7^+,$$
$$r_4 = k_4 Q_{C_6H_{14}} = k_4 K_{p_{C_6H_{14}}} p_{C_6H_{14}} Q_s \quad [A.11]$$
$$C_6H_{15}^+ \rightarrow C_4H_{10} + C_6H_5^+,$$
$$r_5 = k_5 Q_{C_6H_{14}} = k_5 K_{p_{C_6H_{14}}} p_{C_6H_{14}} Q_s. \quad [A.12]$$

Similarly, the overall bimolecular reactions which are combinations of hydride transfer and β-scission steps can be described using the expressions and rates,

$$C_6H_{14} + C_6H_5^+ \rightarrow C_5H_{12} + C_6H_7^+,$$
$$r_6 = k_6 p_{C_6H_{14}} Q_{C_2H_4} = k_6 K_{p_{C_2H_4}} p_{C_6H_{14}} p_{C_2H_4} Q_s \quad [A.13]$$
$$C_6H_{14} + C_6H_7^+ \rightarrow C_3H_8 + C_6H_{13}^+,$$
$$r_7 = k_7 p_{C_6H_{14}} Q_{C_3H_6} = k_7 K_{p_{C_3H_6}} p_{C_6H_{14}} p_{C_3H_6} Q_s \quad [A.14]$$
$$C_6H_{14} + C_6H_5^+ \rightarrow C_4H_{10} + C_6H_9^+,$$
$$r_8 = k_8 p_{C_6H_{14}} Q_{C_2H_4} = k_8 K_{p_{C_2H_4}} p_{C_6H_{14}} p_{C_2H_4} Q_s \quad [A.15]$$
$$C_6H_{14}^+ + C_6H_7^+ \rightarrow C_5H_{12} + C_6H_9^+,$$
$$r_9 = k_9 p_{C_6H_{14}} Q_{C_3H_6} = k_9 K_{p_{C_3H_6}} p_{C_6H_{14}} p_{C_3H_6} Q_s \quad [A.16]$$
$$C_6H_{14}^+ + C_6H_{11}^+ \rightarrow C_5H_{12} + C_6H_{13}^+,$$
$$r_{10} = k_{10} p_{C_6H_{14}} Q_{C_5H_{10}} = k_{10} K_{p_{C_5H_{10}}} p_{C_6H_{14}} p_{C_5H_{10}} Q_s. \quad [A.17]$$

Finally, the overall reaction for isomerization of the feed and its rate is given by

$$C_6H_{14} + C_6H_{13}^+ \rightarrow \text{i-}C_6H_{14} + C_6H_{13}^+,$$
$$r_{11} = k_{11} p_{C_6H_{14}} Q_{C_6H_{12}} = k_{11} K_{p_{C_6H_{12}}} p_{C_6H_{14}} p_{C_6H_{12}} Q_s. \quad [A.18]$$

Now, an overall active site balance gives

total number of free sites
= (total number of sites)
− (total number of occupied sites)

$$Q_s = Q_{acid} - Q_{C_6H_{14}} - Q_{C_6H_{12}} - Q_{C_5H_{10}} - Q_{C_4H_8} - Q_{C_3H_6} - Q_{C_2H_4}; \quad [A.19]$$

substituting for Q_i using the equilibrium relationships of Eq. [A.7] gives

$$Q_s = Q_{acid} - K_{p_{C_6H_{14}}} p_{C_6H_{14}} Q_s - K_{p_{C_6H_{12}}} p_{C_6H_{12}} Q_s - K_{p_{C_5H_{10}}} p_{C_5H_{10}} Q_s - K_{p_{C_4H_8}} p_{C_4H_8} Q_s - K_{p_{C_3H_6}} p_{C_3H_6} Q_s - K_{p_{C_2H_4}} p_{C_2H_4} Q_s \quad [A.20]$$

rearranging

$$Q_s = \frac{Q_{acid}}{1 + K_{p_{C_6H_{14}}} p_{C_6H_{14}} + K_{p_{C_6H_{12}}} p_{C_6H_{12}} + K_{p_{C_5H_{10}}} p_{C_5H_{10}} + K_{p_{C_4H_8}} p_{C_4H_8} + K_{p_{C_3H_6}} p_{C_3H_6} + K_{p_{C_2H_4}} p_{C_2H_4}}. \quad [A.21]$$

Substitution of Q_s in the rate expressions results in the Eley–Rideal form of rate expression for each reaction. The rate expressions that have been implemented are given in Table 1.

REFERENCES

1. Chen, D. T., Sharma, S., Cardona-Martinez, N., Dumesic, J. A., Bell, V. A., Hodge, G. D., and Madon, R. J., *J. Catal.* **136**, 392 (1992).
2. Ho, T. C., Katritzky, A. R., and Cato, S. J., *Ind. Eng. Chem. Res.* **31**, 1589 (1992).
3. Zhao, Y., and Wojciechowski, B. W., *J. Catal.* **144**, 377 (1993).
4. Fogler, H. S., "Elements of Chemical Reaction Engineering," 2nd ed. Prentice-Hall International, Englewood Cliffs, NJ, 1992.
5. Zhao, Y., Bamwenda, G. R., and Wojciechowski, B. W., *J. Catal.* **142**, 465 (1993).
6. Chen, D. T., Sharma, S. B., Fillimonov, I., and Dumesic, J. A., *Catal. Lett.* **12**, 201 (1992).
7. Froment, G. F., and Bischoff, K. B., "Chemical Reactor Analysis and Design," 2nd ed. Wiley, New York, 1990.
8. *J. Phys. Chem. Ref. Data* **17**, Supplement 1 (1988).
9. Parillo, D. J., Gorte, R. J., and Farneth, W. E., *J. Am. Chem. Soc.* **115**, 12441 (1993).
10. Atkins, P. W., "Physical Chemistry." Oxford Univ. Press, London, 1978.
11. Maatman, R. W., Lago, R. M., and Prater, C. D., *Adv. Catal.* **9**, 531 (1957).
12. Zhao, Y., Bamwenda, G. R., Groten, W. A., and Wojciechowski, B. W., *J. Catal.* **140**, 243 (1993).
13. Abbott, J., and Wojciechowski, B. W., *J. Catal.* **107**, 571 (1987).
14. Dumesic, J. A., "The Microkinetics of Heterogeneous Catalysis." Am. Chem. Soc., Washington, DC, 1993.
15. Cardona-Martinez, N., and Dumesic, J. A., *Adv. Catal.* **38**, 149 (1992).
16. Koch, H., and Haaf, W., *Liebigs Ann. Chem.* **618**, 251 (1958).